Observing ^{13}C-^{13}C connectivities at high magnetic field and very high spinning frequencies

Olivier Lafon,[a] Julien Trébosc,[a] Bingwen Hu,‡[a] Gaël De Paëpe[b] and Jean-Paul Amoureux*[a]

[a] *Unit of Catalysis and Chemistry of Solids (UCCS), CNRS-8181, University Lille Nord de France, 59652 Villeneuve d'Ascq, France. Tel: (33) 320434143; E-mail: jean-paul.amoureux@univ-lille1.fr*
[b] *Service de Chimie Inorganique et Biologique (SCIB), UMR-E 3 CEA / UJF-Grenoble 1, Institut Nanosciences et Cryogénie (INAC), F-38054 Grenoble, France; E-mail: gael.depaepe@cea.fr*

Electronic Supplementary Information

I-Numerical simulations

All numerical simulations were performed using Simpson software.[1] The spin system consists of an isolated pair of ^{13}C nuclei. All tensor orientations are related to the peptide plane (*E*) having x_E along N–H and z_E being the normal to the plane. Except for the difference in isotropic chemical shift, which is varied from 0 to 40 kHz, other spin system parameters are typical of a $^{13}C^{\alpha}$-$^{13}C'$ pair within an amino-acid residue.[2] The ^{13}C-^{13}C distance is 154 pm, which corresponds to a dipolar coupling constant, $b_{cc}/(2\pi) = -2.0$ kHz. The Euler angles relating the C–C bond to the peptide plane (*E*) are $\left(\beta_{PE}^{D}, \gamma_{PE}^{D}\right)$= (90, 120.8). All simulations were performed at B_0 = 23.5 T. The CSA tensors are such (CSA_{13C}, η^{CS}, $\alpha_{PE}^{CS}, \beta_{PE}^{CS}, \gamma_{PE}^{CS}$) = (–20 ppm, 0.43, 90, 90, 0) and (76 ppm, 0.90, 0, 0, 94) for C^{α} and C' sites, respectively. The powder averaging used 256 $\{\alpha_{ER},\beta_{ER}\}$ pairs and 11 γ_{ER} angles selected according to the REPULSION algorithm.[3] The rf nutation frequency for $H\text{-}BR2_2^1$ is $\nu_{13C} = \nu_R/2$. The double-quantum filtered (DQF) spectra are obtained using the pulse sequence depicted in Fig.1 with $t_1 = 0$. The DQF efficiency is calculated as the ratio of the integral of the one-dimensional (1D) DQF spectrum to the integral of the 1D ^{13}C spectrum obtained after a $\pi/2$-pulse excitation.

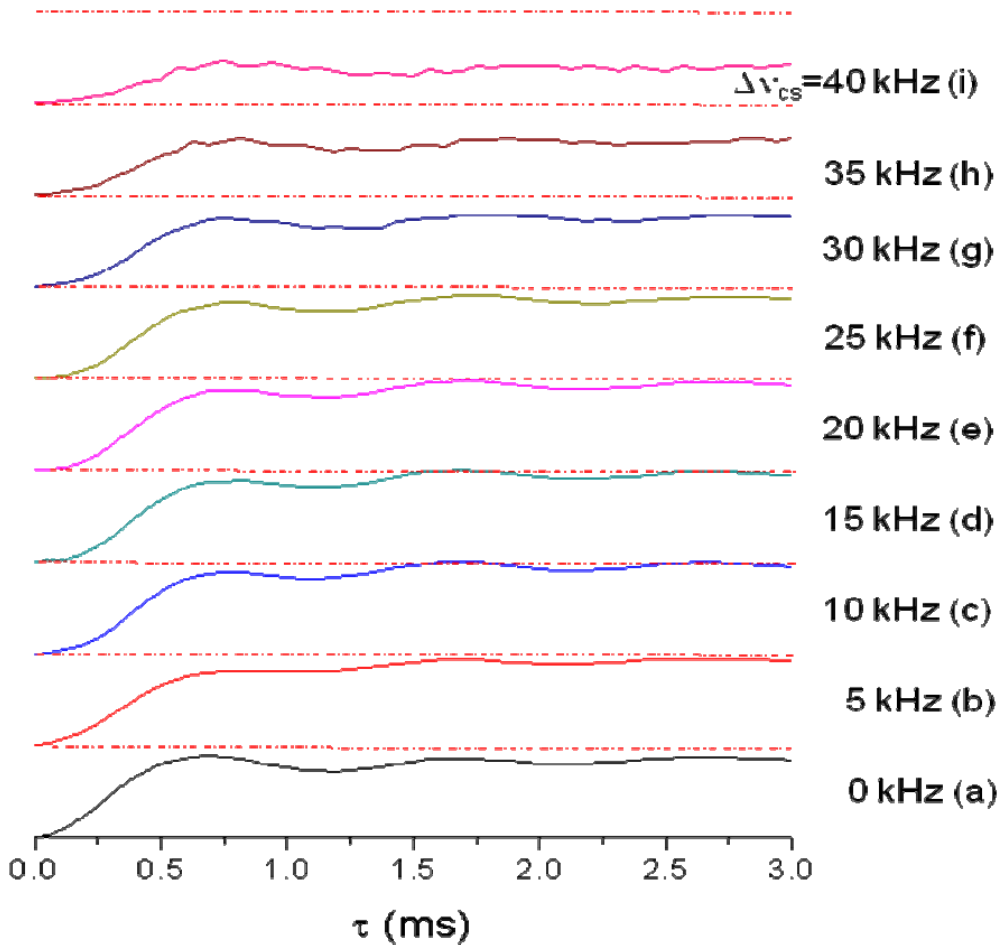

Fig.S1. Simulated DQF build-up curves for one ^{13}C-^{13}C isolated pair at ν_R = 64 kHz and B_0 = 23.5 T. The rf-irradiation is placed in the middle of the two carbon resonances, which are separated by $\Delta\nu_{cs}$ = (a) 0, (b) 5, (c) 10, (d) 15, (e) 20, (f) 25, (g) 30, (h) 35 kHz. The dash dot line denotes the maximum efficiency, which is always equal to 23%. On resonance ($\Delta\nu_{cs}$ = 0 kHz), the maximum DQF efficiency is reached at $\tau^{opt} \approx 700$ µs. For larger $\Delta\nu_{cs}$ differences, the τ^{opt} values double.

II-Experimental section

The ^{13}C chemical shifts were referenced from tetramethylsilane (TMS). The spectra displayed in Fig. 3 and 4 were acquired using the pulse sequence displayed in Fig.1. The quadrature along the indirect dimension was obtained using States-TPPI procedure.[4] Pre-saturation pulse trains were applied on both ^1H and ^{13}C channels to ensure identical conditions between each transient and to eliminate the thermal equilibrium ^{13}C magnetization, which does not originate from ^1H magnetization. The L-[U-^{13}C]-histidine·HCl sample was purchased from CortecNet. The experiments on L-[U-^{13}C]-histidine·HCl and [U-^{13}C]-YajG were performed on narrow-bore Bruker AVANCE-III spectrometers operating at B_0 = 23.5 and 21.14 T, respectively. The ≈ 1.5 µl samples were spun at ν_R = 60 kHz in a double-resonance 1.3 mm MAS probe.

For L-[U-^{13}C]-histidine·HCl, the rf nutation frequency of ^{13}C and ^1H hard-pulses, $\nu_{1,HP,13C}$ and $\nu_{1,HP,1H}$, were 90 and 111 kHz. During the $^1H \rightarrow {}^{13}C$ CP transfer of τ_{CP} = 5 ms, the ^1H rf nutation frequency, $\nu_{1,CP,1H}$, was ramped from 140 to 160 kHz, while the ^{13}C nutation frequency, $\nu_{1,CP,13C}$, was 90 kHz. The ^1H–^{13}C dipolar couplings were removed by SPINAL-64 decoupling during t_1 and t_2 periods with ^1H nutation frequency of 15 kHz and a pulse length of 30 µs.[5,6] For [U-^{13}C]-YajG, we used $\nu_{1,HP,13C}$ = 131 kHz and $\nu_{1,HP,1H}$ = 66 kHz. During the $^1H \rightarrow {}^{13}C$ CP transfer of τ_{CP} = 1.6 ms, the ^1H rf nutation frequency, $\nu_{1,CP,1H}$, was ramped from 35 to 39 kHz, while the ^{13}C nutation frequency, $\nu_{1,CP,13C}$, was 97 kHz. The ^1H–^{13}C dipolar couplings were removed by SPINAL-64 decoupling during t_1 and t_2 periods with ^1H nutation frequency of 15 kHz and a pulse length of 30 µs.

With such low rf frequency, heating of the sample mainly arises from air friction onto the rotor wall during spinning. Temperature inside the sample under MAS was evaluated using lead nitrate as a NMR thermometer.[7] Although the

thermocouple located inside the stator does not show any significant temperature increase between 0 and 60 kHz spinning speed, $Pb(NO3)_2$ ^{207}Pb chemical shift drift shows that using room temperature (20° C) bearing and drive compressed air flow without temperature regulation, the sample temperature increases by 30° C to reach a maximum of 50° C at 60 kHz MAS with a 15° C temperature gradient across the rotor. Thus active cooling is required to keep the protein in a safe environment. Temperature regulation is performed independently from bearing and drive airflow by a third variable temperature (VT) air input. Cold air (as low as -70° C) produced by a Bruker BCU-Xtreme device is heated up and blown on the rotor. Thermocouple measures results from VT air mixing with bearing and drive air required for 60 kHz spinning speed. A temperature down to -35° C inside the stator has been measured with a VT air flow of 1600L/h. Under such conditions lead nitrate shows that sample temperature then lies below 25° C. Figure S2.a) summarizes temperature evolution as a function of spinning speed without regulation and figure S2.b) temperature evolution as a function of thermocouple measured temperature using active regulation with VT gas flow of 1600L/h under 60 kHz MAS.

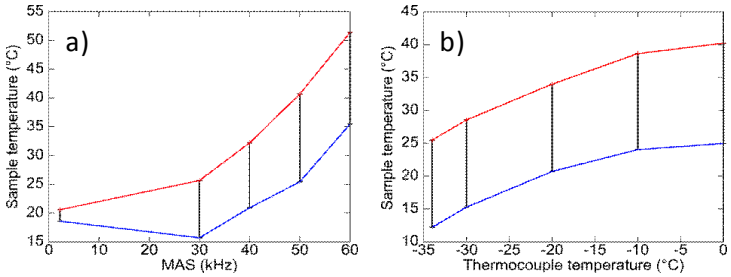

Fig.S2. a) Temperature as a function of spinning speed without VT regulation. b) Temperature calibration of thermocouple under 1600L/H VT gas flow. Error bars represent the temperature gradient across the rotor.

III-Data processing of YajG spectra

In the following, the angular frequencies along indirect and direct dimensions are denoted Ω_1 and Ω_2, respectively. The data processing was performed using matNMR toolbox,[8] within Matlab environment.[9] The covariance transform and time-domain regularization were implemented in matNMR as Matlab programs.[10] The time-domain data set, $s(t_1,t_2)$, was zero-filled to 2048 complex points along t_2 dimension and apodized using a decreasing exponential with a decay rate of λ = 100 Hz. Non-uniformly sampled (NUS) data set was generated by selecting a limited number, N_1 (States), of t_1 increments according to an exponentially decaying density probability.[11] For conventional Fourier Transform (FT) processing, a decreasing exponential with a decay rate of λ = 100 Hz was applied along t_1 dimension. The two mixed time-frequency 2D matrices were zero-filled along t_1 dimension to 2048 increments prior to FT. For covariance (Cov) processing, the cosine- and sine-modulated mixed time-frequency 2D matrices, $Re[s_c(t_1,\Omega_2)]$ and $Re[s_s(t_1,\Omega_2)]$, were first sheared in the t_1 time domain in order to convert the t_1 dimension from DQ to SQ.[12] Then, these data sets were regularized by the addition of diagonal signals using a regularization factor, α = 100, and a decay rate constant, λ = 5 Hz. The covariance spectrum was calculated using singular value decomposition (SVD) algorithm,[13] and the uninformative diagonal peaks were subtracted. To conclude, the symmetrical covariance spectra were sheared back along the indirect dimension in order to obtain conventional DQ-SQ representations, which can be easily compared with the FT 2D spectra.

Fig.S3 shows a comparison of the full DQ-SQ ^{13}C *D*-HOMCOR spectra of [U-^{13}C]-YajG using different sampling and processing methods. Expanded regions and extracted columns of these spectra are displayed in Fig.S4. The comparisons of Figs.S3a and b as well as S4a and d show that the combination of Cov with a regularization method allows a reliable reconstruction of DQ-SQ *D*-HOMCOR 2D spectra, even for 192-amino-acid proteins displaying hundreds of ^{13}C signals. In particular, this procedure does not reintroduce uninformative DQ diagonal peaks (with $\Omega_1 = 2\Omega_2$). In addition, the comparison of Figs.S4a-c and d-f demonstrates that Cov treatment enhances the spectral resolution along the indirect dimension by endowing the indirect dimension with the spectral resolution of the direct dimension. Furthermore, regularized Cov treatment can be employed for the spectral estimate of NUS DQ-SQ *D*-HOMCOR data set. The comparison of Figs.S4d-f and g-i shows no significant degradation in spectral resolution when decreasing the number of t_1 increment from 143 to 48, i.e. a reduction in experiment time by a factor of 3. Nevertheless, the reduction in experiment time inevitably entails a reduction in S/N ratio since the sensitivity is an increasing function of the number of sampled data points. By observing the line-shapes one observes an interesting phenomenon: there is a 'slopping' of the cross-peaks in Fig.S4d,g, which cannot be observed in Fig.S4a due to the resolution decrease. This 'slopping', which is related to the superposition of identical amino acid signals in different surroundings, is not observable in histidine (Fig.3), where each carbon species is only related to a single surrounding. This 'slopping' of the cross-peaks is similar to that already observed with refocused INADEQUATE spectra of disordered solids.[14]

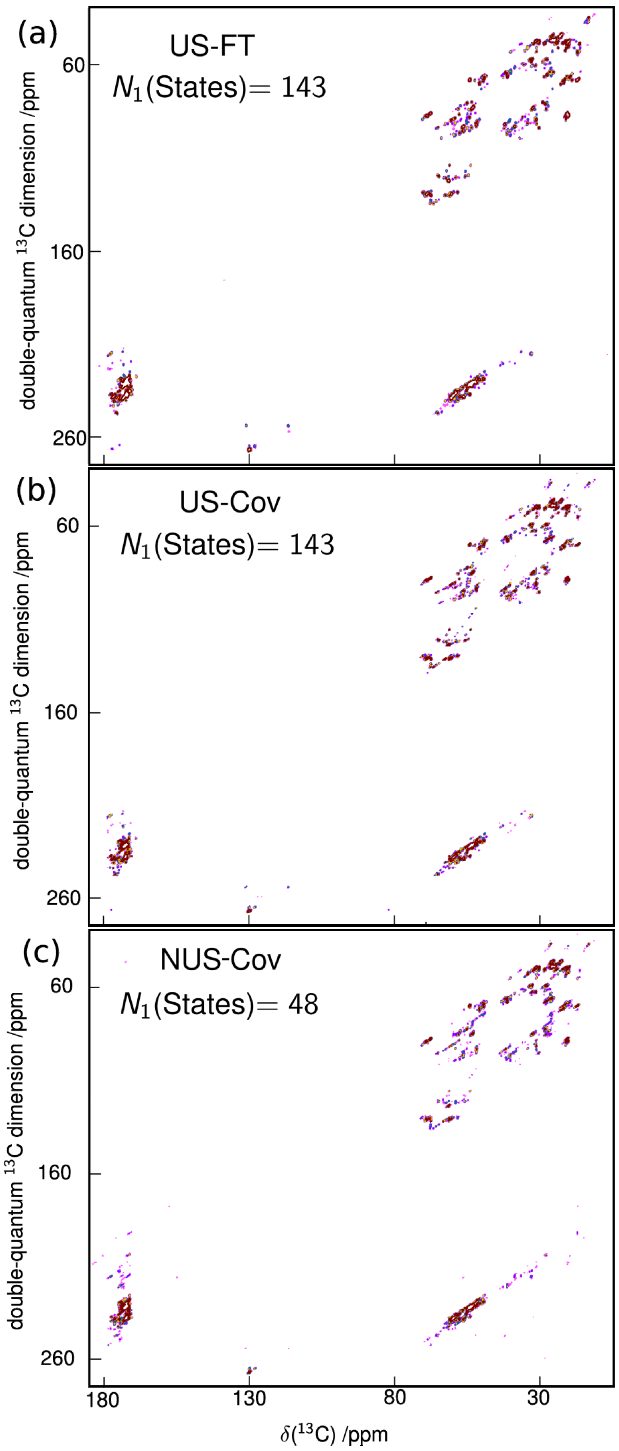

Fig.S3. Comparison of DQ-SQ ^{13}C *D*-HOMCOR 2D spectra of [U-^{13}C]-YajG obtained using different sampling and processing methods. The experimental data set is the same as that used in Fig.4. The DQ-SQ data were acquired using $\mathrm{H-BR2}_2^1$ recoupling at 21.14 T and ν_R = 60 kHz. Spectrum b is identical to the full spectrum displayed in Fig.4. (a) Spectrum obtained by uniform sampling and conventional Fourier transform along indirect F_1 dimension (US-FT) using N_1 (States) = 143. (b) Spectrum obtained by uniform sampling and covariance transform along indirect F_1 dimension (US-Cov) using N_1 (States) = 143. (c) Spectrum obtained by non-uniform sampling and covariance transform along indirect F_1 dimension (NUS-Cov) using N_1 (States) = 48. Additional details on the processing methods are given in the data processing section.

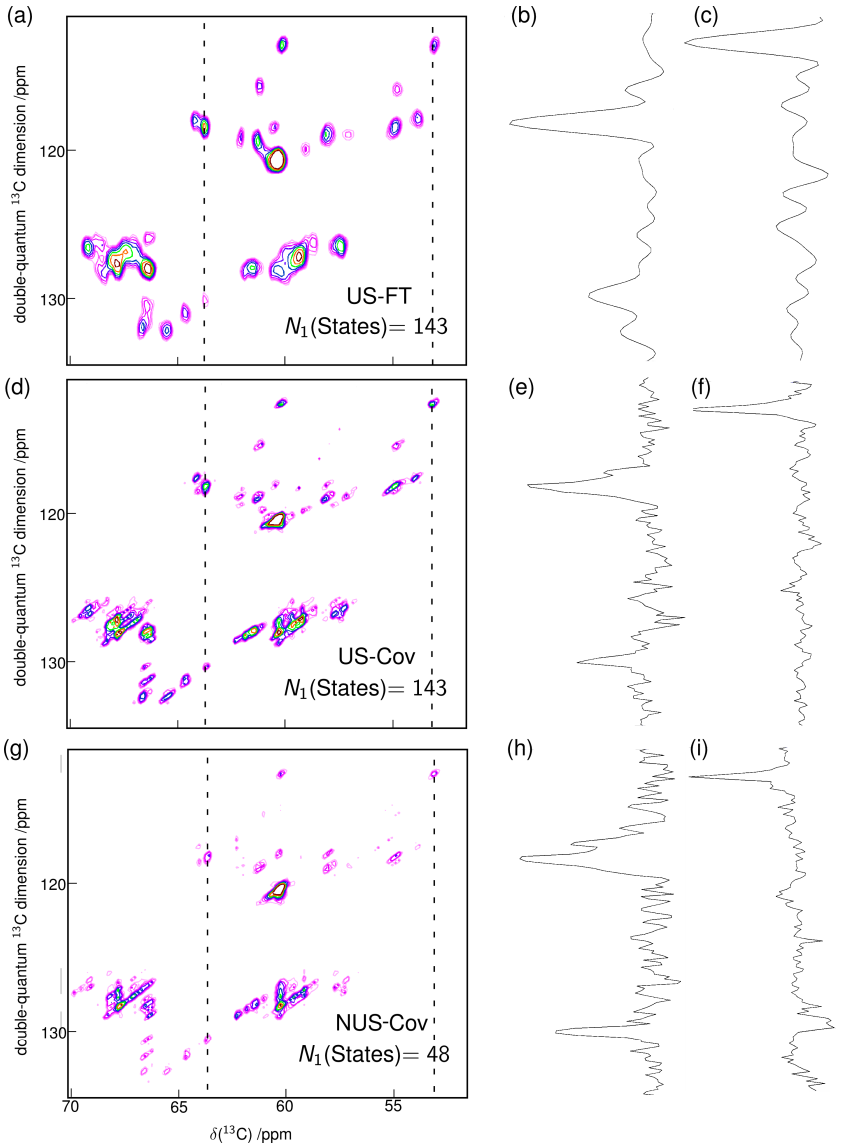

Fig.S4. Comparison performed for the same selected region and the same two columns of DQ-SQ ^{13}C *D*-HOMCOR spectra of [U-^{13}C]-YajG obtained using different sampling and processing methods: (a-c) US-FT with N_1 (States) = 143, (d-f) US-Cov with N_1 (States) = 143, (g-i) NUS-Cov with N_1 (States) = 48. (a,d,g) The selected region is the one framed in the full spectrum displayed in Fig.4. Spectra a, d and g were extracted from the full 2D spectra, shown in Fig.S2a, b and c respectively. The positions of columns at δ_{13C} = 63.8 and 52.9 ppm in SQ dimension are shown as dashed lines. The slices extracted from the regions exposed on the left are shown in (b,e,h) for δ_{13C} = 63.8 ppm, and in (c,f,i) for δ_{13C} = 52.9 ppm. For the three 2D spectra, the same line broadening of 100 Hz was applied along the two dimensions.

1 M. Bak, J.T. Rasmussen, N.C. Nielsen, *J. Magn. Reson*. 2000, **147**, 296.
2 M. Bak, R. Schultz, T. Vosegaard, N.C. Nielsen, *J. Magn. Reson*. 2002, **154**, 28.
3 M. Bak, N.C. Nielsen, *J. Magn. Reson*. 1997, **125**, 132.
4 D. Marion, M. Ikura, R. Tschudin, A. Bax *J. Magn. Reson.* 1989, **85**, 393.
5 B.M. Fung, A.K. Khitrin, K. Ermolaev, *J. Magn. Reson*. 2000, **142**, 97.
6 M. Kotecha, N.P. Wickramasinghe, Y. Ishii, *Magn. Reson. Chem.* 2007, **45**, S221.
7 A. Bielecki, D. P. Burum, *Journal of Magnetic Resonance, Series A* 1995, **116** 215-220
8 J.D. van Beek, *J. Magn. Reson.* 2007, **187**, 19.
9 Mathworks Inc. www.mathworks.com
10 O. Lafon, B. Hu, P. Lesot, J.-P. Amoureux, *Chem. Eur. J.* in press : DOI :10.1002/chem.201100461.
11 J. Barna, E.D. Laue, M.R. Mayger, J. Skilling, S.J.P. Worrall, *J. Magn. Reson.* 1987, **73**, 69.
12 R.R. Ernst, G. Bodenhausen, A. Wokaun, *Principles of Nuclear Magnetic Resonance in One and Two Dimensions*, Oxford University Press, New-York, 1987.
13 N. Trbovic, S. Smirnov, F. Zhang, R. Brüschweiler, *J. Magn. Reson.* 2004, **171**, 277.
14 D. Sakellariou, S.P. Brown, A. Lesage, S. Hediger, M. Bardet, C.A. Meriles, A. Pines, L. Emsley, J. Am. Chem. Soc. 2003, 125, 4376.